Advances in Science and Technology Research Journal

Advances in Science and Technology Research Journal 2024, 18(5), 258–267
https://doi.org/10.12913/22998624/191110
ISSN 2299-8624, License CC-BY 4.0

Received: 2024.06.18
Accepted: 2024.07.20
Published: 2024.08.01

Optimizing Amorphous Silica Recovery from Rice Husk Cultivated under Different Soils for Supplementary Cementitious Material Application

Pham Viet Hung[1*], Ve Quoc Linh[1], Vo Cong Anh[1], Do Thanh Tien[1], Ngo Quy Tuan[1], Tran Duc Hanh[1], Dao Van Phu[1], Nguyen Thi Thanh[1], Pham Xuan Phuong[1], Pham Thi Thanh Phuc[1]

[1] Faculty of Engineering and Technology, University of Agriculture and Forestry, Hue University, Thua Thien Hue 530000, Vietnam

* Corresponding author's e-mail: pvhung.huaf@hueuni.edu.vn

ABSTRACT

Amorphous silica (a-SiO_2), found in rice husk ash, is a valuable material due to its high silica content, large surface area, excellent pozzolanic properties, and strong binding ability with cement. These characteristics make it ideal for use as a supplementary cementitious material and a sustainable alternative for the partial replacement of ordinary Portland cement. This study aims to optimize the recovery process of amorphous silica from rice husks cultivated under various soil conditions (normal, drought, saline, and acidic soils), which are experiencing significant fluctuations due to climate change in many rice-producing countries. Experiments were conducted on rice husks under different pyrolysis conditions at temperatures of 700 °C, 800 °C, and 900 °C, with varying calcination durations. Through comprehensive analysis using Scanning electron microscopy (SEM) and X-ray diffraction (XRD), along with the evaluation of amorphous silica recovery efficiency, we identified the optimal conditions for producing amorphous silica from rice husks. The analysis revealed that the highest recovery efficiency was achieved at a pyrolysis temperature of 700 °C for 1 hour. Under these conditions, the recovery efficiencies were 87.9% for normal soil RHA, 96.5% for saline soil RHA, 94.8% for drought soil RHA, and 95.6% for acidic soil RHA. The phase structure, surface morphology, and particle size of the RHA-derived amorphous silica, ground to micrometer sizes, were found to be similar to commercial products such as ordinary Portland cement and silica fume. This study provides a foundation for scaling up the production of amorphous silica from rice husk ash on an industrial scale, considering the relationship between optimal recovery efficiency and the origin of the rice husk ash, thus contributing to the development of environmentally friendly construction materials.

Keywords: rice husk, rice husk ash, pyrolysis, amorphous silica, recovery efficiency, supplementary cementitious material.

INTRODUCTION

Recently, the need to build infrastructure and housing projects has been increasing dramatically with strong economic development and continuous population growth. Most construction materials are sourced from nature, which consumes energy and has high costs. The waste from the exploitation and production of construction materials causes serious environmental pollution. The commonly used construction material is ordinary Portland cement (OPC), which has high mechanical strength and durability [1]. However, the cement production process consumes enormous energy and has a very high investment cost. Furthermore, this industrial production emits a large amount of CO_2, which accounts for 5-8% of global CO_2 emissions [2–4]. Therefore, the need to find low-cost, energy-efficient, and eco-friendly materials to replace traditional cement is very urgent.

Rice husk ash (RHA) obtained from the pyrolysis process has a high amount of amorphous silica content with a large surface area, good pozzolanic properties, and linking ability with aggregates like traditional cement [5–8]. Therefore, research on using RHA as a partial matter for enhancing the performance of cement-based materials has attracted many scientists [9, 10]. RHA with a high amorphous silica content increased the chemical activity (or the pozzolanic reaction between SiO_2 and CH) [11, 12]. Therefore, this promotes the hydration of cement in the later stage and improves the resistance to chloride ion penetration of cement-based materials [13, 14]. Generally, the compatible pozzalanic reaction between RHA and cement is detected when RHA contains 85–95% amorphous silica [15]. Furthermore, the strength of concrete is improved due to RHA containing amorphous silica [16, 17]. Thus, the production of RHA with a high percentage of amorphous silica is necessary for green material construction. Therefore, RHA-derived amorphous silica is of interest as a sustainable material with the potential to partially replace cement or serve as supplementary cementitious materials (SCMs) for construction applications. The RHA production process with a high amount of amorphous silica depends on the burning method, rice husk characteristics, pretreatment of rice husk before incineration, pyrolysis temperature, and time [15, 18]. An open-field burning of rice husk without a controlled temperature leads to RHA with a low carbon content [19, 20]. Otherwise, some previous studies recommended the complete incineration of rice husk at 500–750 °C obtain the RHA with the highest amorphous silica [18, 21, 22]. However, when the combustion temperature reached 600 °C, the crystalline transformation to tridymite and cristobalite happened [23]. According to Bazargan et al. [24], the chemical composition of RHA can influence the pyrolysis temperature at which the phase transition occurs. The pretreatment of rice husk, such as acid leaching and water soaking, was also a required method to achieve a high specific surface area and purity of amorphous silica [25–28]. The characteristics of rice husk were another factor that impacted the production of amorphous silica [29]. The high impurity in rice husks may require a more stringent controlled temperature during pyrolysis to avoid the crystalline transition phase [30, 31].

In Thua Thien Hue province, approximately 54.1 thousand hectares cultivate rice, and about 620.0 thousand tons of dry straw are discharged annually. Most rice-growing areas in Phong Dien, Quang Dien, Huong Tra, Phu Vang, and Phu Loc districts are adjacent to more than 70 km of Tam Giang lagoon. Therefore, the phenomenon of saltwater intrusion in areas of Thua Thien Hue province is happening more and more, affecting the rice cultivation process. According to statistics from the Department of Agriculture and Rural Development of Quang Dien district, the area of rice land affected by saltwater intrusion was 530 hectares in 2014. Similarly, the process of saline intrusion affecting the area of rice cultivation land in Phu Vang district is also very significant. Furthermore, due to harsh climatic conditions, most rice cultivation soil has a low pH (or acid sulphate soil), and most rice cultivation soil lacks irrigation water. Most rice husks are used for different purposes with low economic value, like fertilizer, animal feed, or burning matter. These purposes also cause environmental pollution and increase global warming. Therefore, converting rice husk into RHA with a high ratio of amorphous silica seems to be the better solution to lessen gas emissions and enhance economic value.

This study aims to optimize the recovery process of amorphous silica from the rice husk cultivated under different soil conditions, which are experiencing significant fluctuations due to climate change in many rice-producing countries. The research also identifies how soil types influence the characteristics of rice husk and affect the quality and yield of amorphous silica, as well as its suitability as a supplementary cementitious material. These findings support the development of sustainable SCMs from agricultural by-products, providing feasible solutions to enhance the performance and durability of cementitious materials while promoting environmentally friendly practices in agriculture and construction.

MATERIALS AND METHODS

Materials

Rice husks of the most popular type of rice in Thua Thien Hue province, Huong Thom 1 (HT1), were collected in 2022 for research. To investigate the difference in RHA properties after the pyrolysis process, four rice husks of HT1 cultivated in four conditions, including normal, saline, acid, and drought cultivation conditions, were selected as raw material sources. Rice husk samples are washed, naturally dried, and dried to a moisture content of 10–15% before pyrolysis according to the previous method [32]. Rice husks from rice cultivated under normal, drought, saline, and acidic soil conditions are abbreviated as "normal soil RHA," "drought soil RHA," "saline soil RHA," and "acidic soil RHA," respectively.

Experimental methods

The preparation and pyrolysis processes of rice husks are illustrated in Figure 1. The rice husks are rinsed to eliminate waste, and then the wet rice husks are dried in a drying cabinet to achieve the desired humidity before the pyrolysis stage. In each pyrolysis condition, four sealed ceramic pots of different rice husks are pyrolyzed at the same time using a specialized furnace, the Nabertherm N7/H/B400, made in Germany. The pyrolyzed temperatures were 700 °C, 800 °C, and 900 °C, and the pyrolyzed duration was 1 hour and 2 hours, respectively. To obtain the target pyrolysis temperature, the heating process is controlled by the slow pyrolysis heating rate of 10 °C/min at room temperature. After a 1- or 2-hour pyrolysis process, leave the RHAs out in the ambient conditions to cool down naturally.

The RHA properties of four different types of rice husk were analyzed by scanning electron microscope (SEM) and X-ray diffraction (XRD). SEM is used to analyze the surface structure of RHA by using an SEM device (Jeol, Japan). The XRD patterns of RHAs were achieved using a Bruker D8 Advance Eco operated at 2 Theta between 10° and 80°. The operating conditions for the pyrolysis process are summarized in Table 1.

RESULTS AND DISCUSSION

The effect of pyrolysis temperature

Figures 2, 3, 4, and 5 revealed the inside layer morphology of 4 RHA samples cultivated in different conditions, including normal soil, saline soil, drought soil, and acidic soil. The pyrolysis temperature and time were 700 °C and 1 hour, respectively. As can be seen from the SEM images in those figures, the surface structures of normal soil's RHA and saline soil's RHA had a higher void fraction (or porous structure) than those of drought soil's RHA and acidic soil's RHA. It

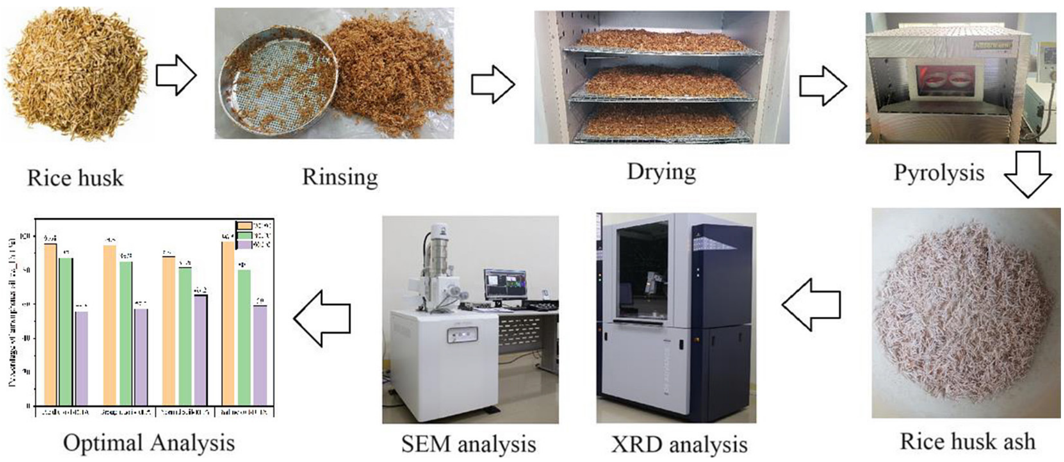

Figure 1. The experimental setup for determining the properties of RHAs

Table 1. Operating conditions for the pyrolysis process

Types of rice husk	Pyrolysis temperature (°C)	Pyrolysis heating rate (°C/min)	Pyrolysis duration (hour)
Acidic soil Drought soil Normal soil Saline soil	700	10	1
	800		
	900		
Acidic soil Drought soil Normal soil Saline soil	700		2
	800		
	900		

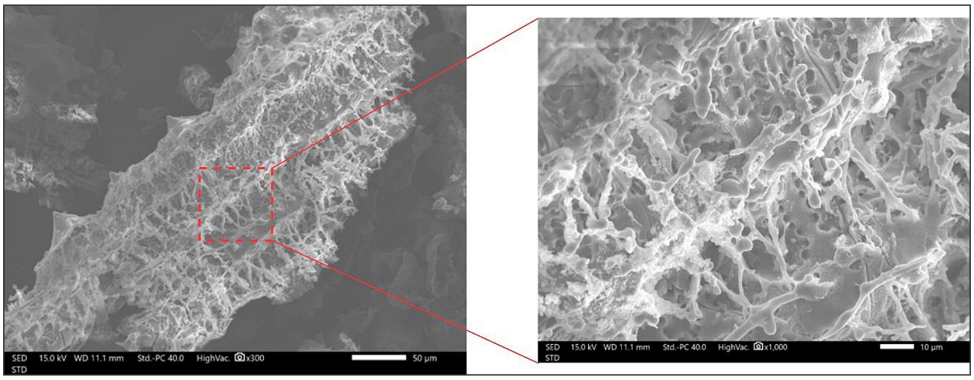

Figure 2. Morphology of the inner surface of RHA cultivated in normal soil

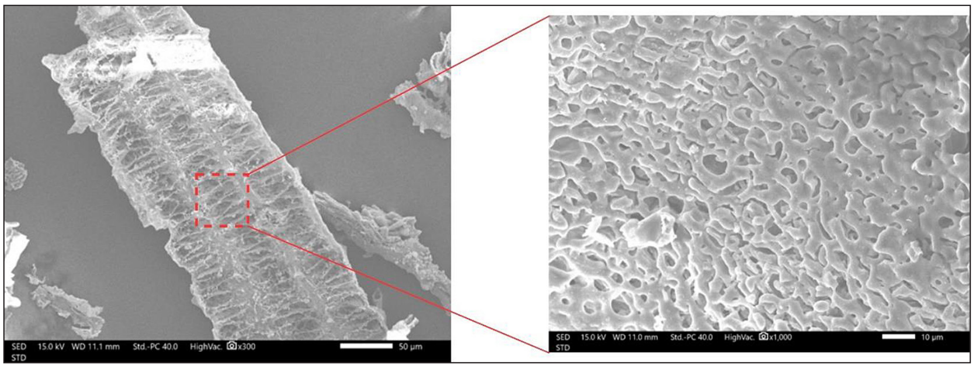

Figure 3. Morphology of the inner surface of RHA cultivated in saline soil

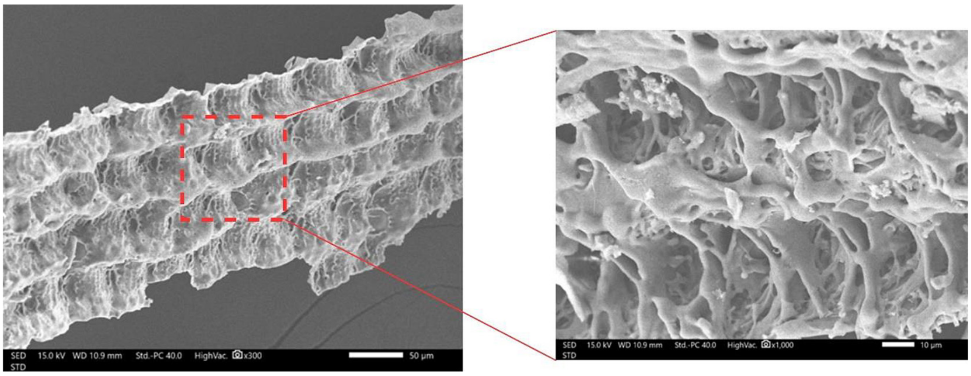

Figure 4. Morphology of the inner surface of RHA cultivated in drought soil

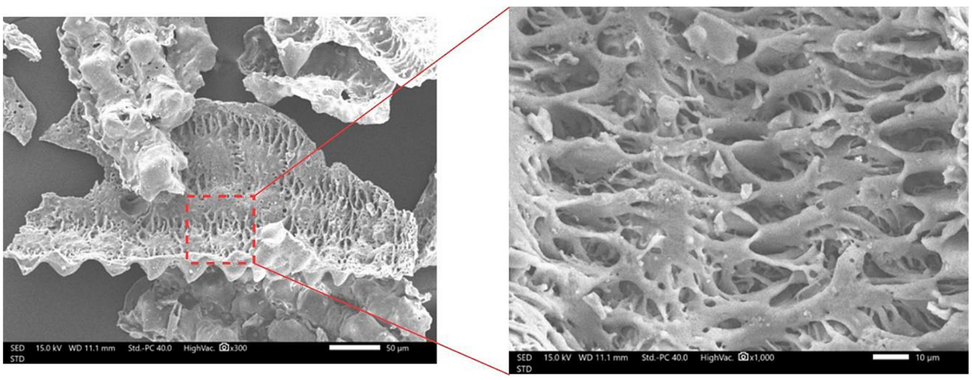

Figure 5. Morphology of the inner surface of RHA cultivated in acidic soil

means the rice husks cultivated in normal and saline soil have lower pyrolysis temperatures than those planted in drought and acidic soil.

XRD patterns of 4 RHAs at different pyrolysis temperatures are shown in Figure 6. At 700 °C and 1 – hour pyrolysis time, there was a similar XRD pattern for 4 RHAs. It is observed that broad diffused peaks with maximum intensity at around 2θ = 22° occurred (Figure 6a). Bakar et al. also determined the same XRD patterns for acid-leached silica and un-leached silica when the broad diffused peaks occurred at 2θ = 22° when the combustion temperatures ranged from 500 °C to 900 °C [33]. It means the amorphous silica is formed at this range of pyrolysis temperature. However, some sharp peaks are observed at 2θ = 26.6° and 2θ = 20.7° in the case of normal soil's RHA and saline soil's RHA (Figure 6a). Therefore, a crystalline transformation occurred in those RHA samples at 700 °C pyrolysis temperature in a 1-hour pyrolysis time. Furthermore, the XRD patterns from Figure 6b, c revealed that the crystalline transformation rose when the pyrolysis temperature was between 800 °C and 900 °C, and those experimental results

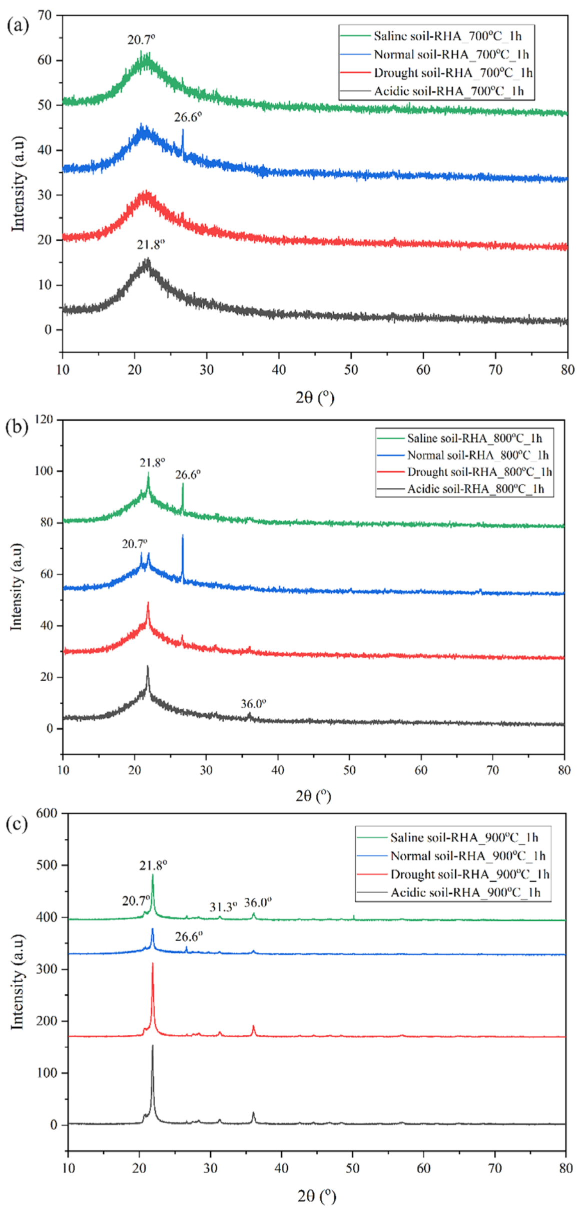

Figure 6. XRD patterns of 4 different RHAs at: (a) 700 °C; (b) 800 °C; (c) 900 °C in 1-hour pyrolysis duration

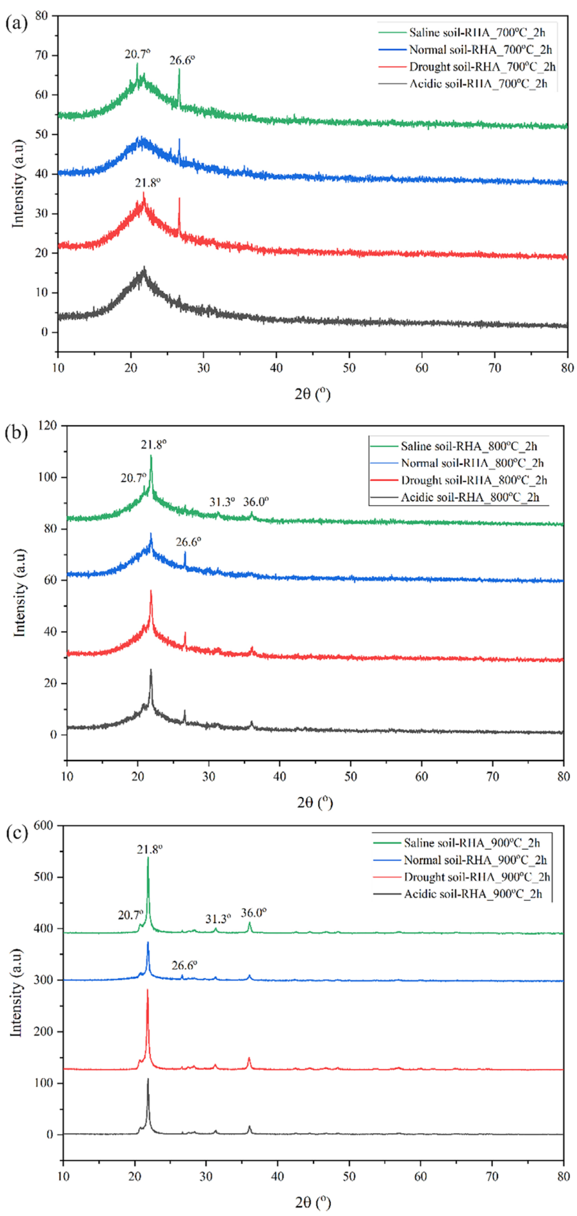

Figure 7. XRD patterns of 4 different RHAs at: (a) 700 °C; (b) 800 °C; (c) 900 °C in 2-hour pyrolysis duration

were coincident with the previous studies [34, 35]. This indicates the recovery efficiency of amorphous silica decreased as the pyrolysis temperature rose from 700 °C to 900 °C [36]. Otherwise, Figure 6 also shows that the pyrolysis temperature for normal and saline soil's rice husk needs to be lower than 700 °C to obtain a better ratio of amorphous silica. On the other hand, 700 °C was the appropriate pyrolysis temperature for the amorphous silica formation in the case of drought and acidic soil rice husk.

Effect of pyrolysis time

Figure 7 revealed the XRD patterns of 4 different RHAs at a pyrolysis temperature of 700–900 °C in a 2-hour duration. From Figures 6 and 7, the recovery efficiency of amorphous silica dropped as the pyrolysis time was longer. According to Greenwood and Earnshaw [32], the longer pyrolysis time is mainly due to the phase transformation to quartz, tridymite, and cristobalite. This conclusion was also proven in the previous study [36]. At 700 °C pyrolysis temperature, the crystalline transformation occurred more and more when the residence time of drought and acidic soil's rice husks in the furnace was longer.

The recovery efficiency of amorphous silica

The recovery efficiency of amorphous silica relates to the calculation of the percentage of crystallinity silica (PCS) that was mentioned in Equation 1 [37]. Therefore, the percentage of amorphous silica (PAS) can be determined in Equation 2.

$$PCS = \frac{ACP}{ACAP} \times 100\% \tag{1}$$

where: ACP – area of all crystalline peaks, ACAP – area of all the crystalline and amorphous peaks.

$$PAS = 100\% - PCS \tag{2}$$

Figures 8 and 9 show that the recovery efficiency of amorphous silica dropped as the pyrolysis temperature rose from 700 °C to 900 °C. As can be seen from Figure 8, the amorphous silica recovery from the pyrolysis of acidic, drought, normal, and saline soil's rice husk at 900 °C decreased by nearly 42%, 40%, 26%, and 44%, respectively, in comparison with at 700 °C. Furthermore, the drop in amorphous silica recovery was quite larger when the pyrolysis process was longer at the same pyrolysis temperature, as shown in Figures 8 and 9. However, the effect of pyrolysis time on the amorphous silica recovery

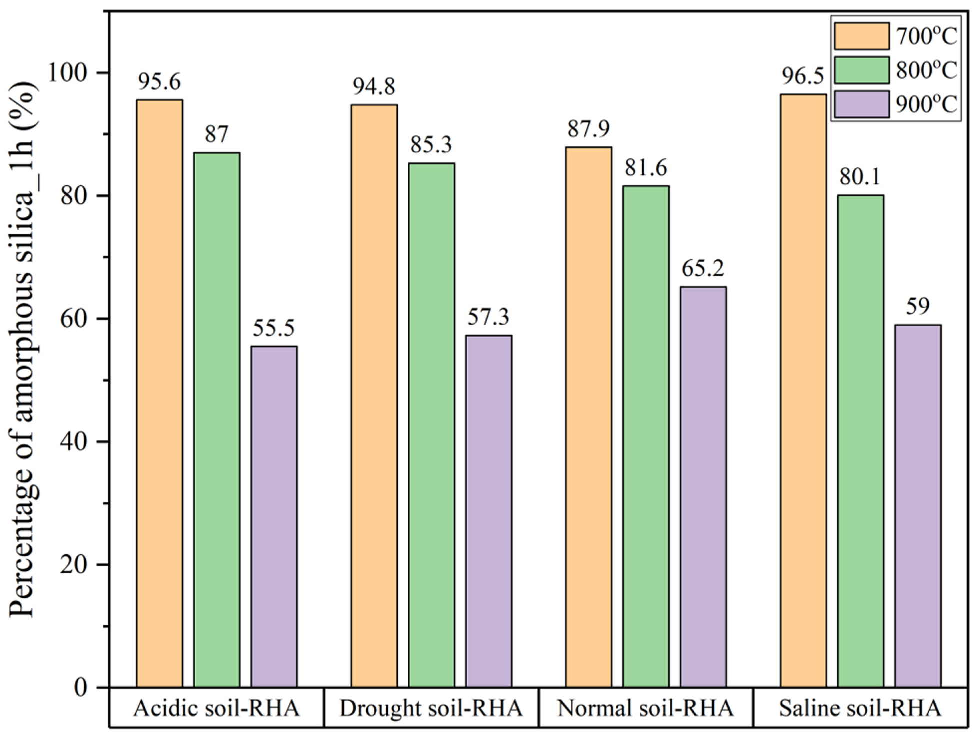

Figure 8. The recovery efficiency of amorphous silica from different types of rice husk in 1-hour pyrolysis time duration at various pyrolysis temperature

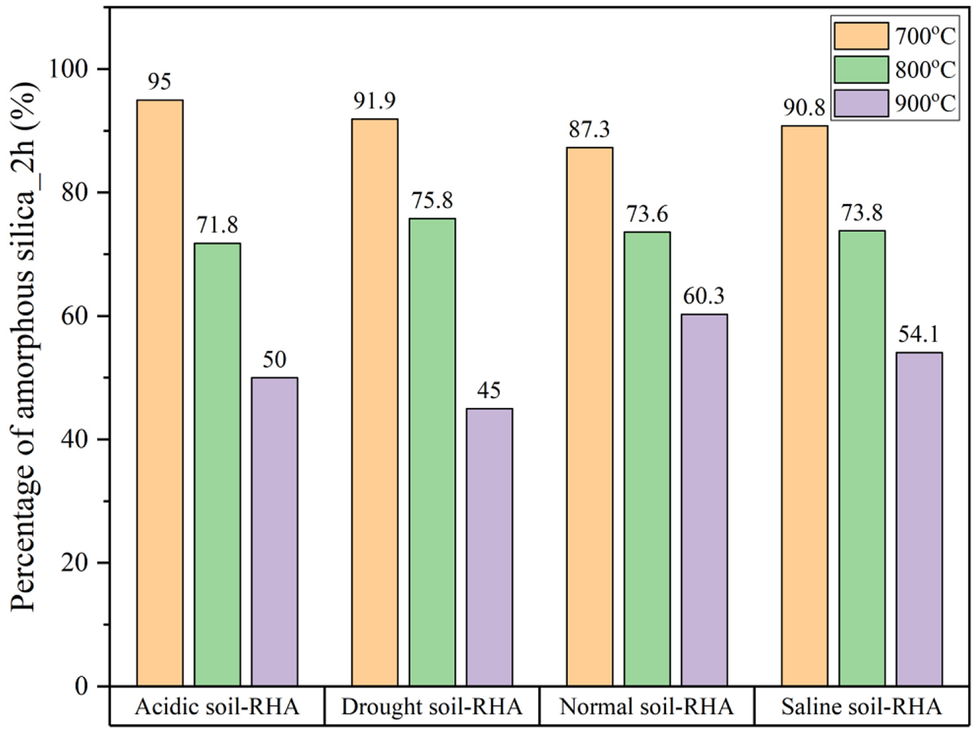

Figure 9. The recovery efficiency of amorphous silica from different types of rice husk in 2-hour pyrolysis time duration at various pyrolysis temperature

efficiency was less significant than the effect of pyrolysis temperature [38, 39].

Comparison to commercial products

The efficiency analysis results for the recovery of amorphous silica from RHA originating from different soil types indicate that optimal conditions are achieved at a pyrolysis temperature of 700 °C for 1 hour. For further evaluation, with the goal of partially replacing OPC and due to its similarity to SF, the phase structure and surface morphology of the four types of RHA-derived amorphous silica were compared with samples of commercial products, namely OPC and SF. The XRD patterns of the OPC and SF samples are shown in Figure 10. The XRD patterns of RHA-derived amorphous silica are similar to those of the SF sample, while the OPC sample is characterized by the presence of not only silica but also various metal oxides in its composition.

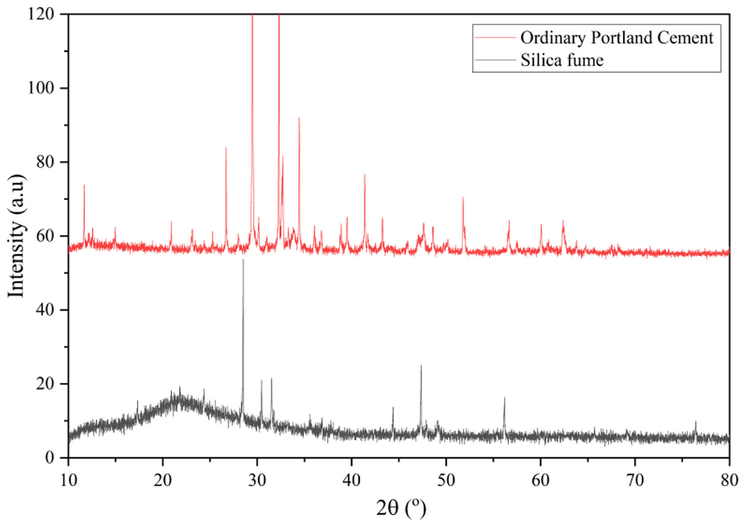

Figure 10. XRD patterns of typical OPC and SF samples

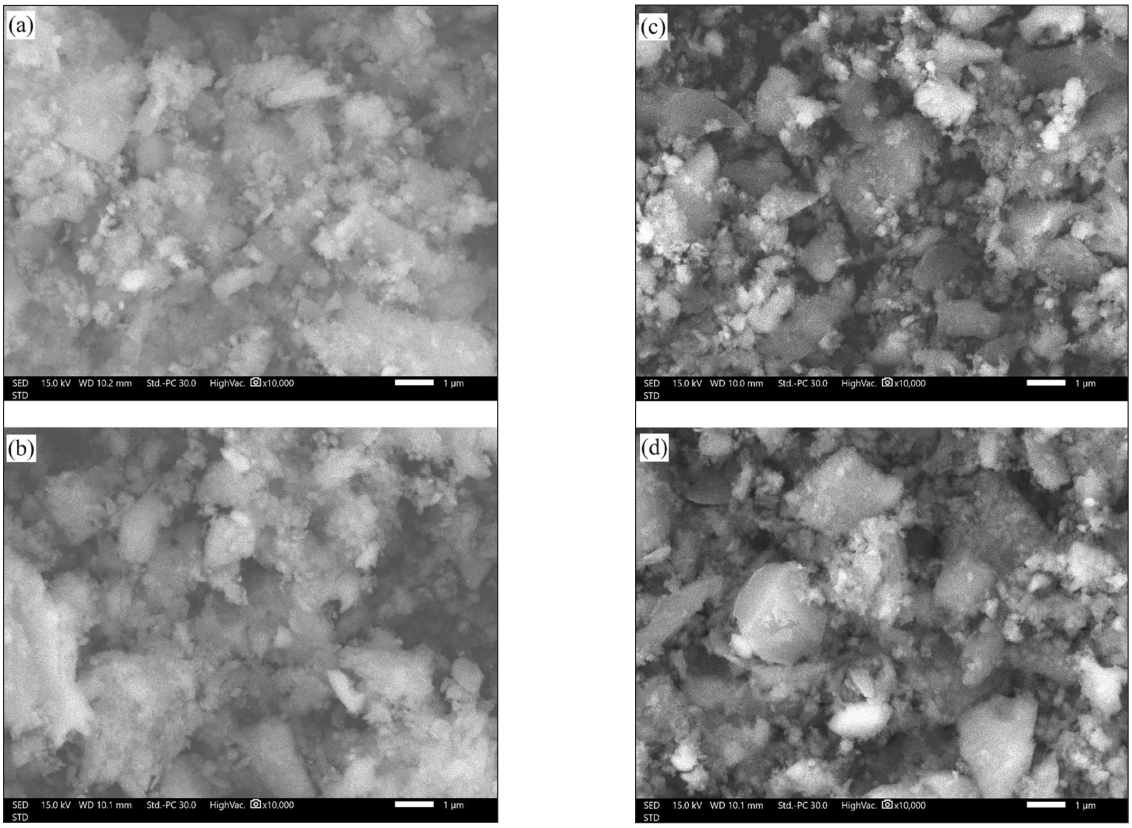

Figure 11. Morphology of RHA samples in microparticle size from: (a) normal soil RHA, (b) saline soil RHA, (c) drought soil RHA, and (d) acidic soil RHA

To evaluate the surface morphology and check particle size, these four types of RHA amorphous silica were reduced to micrometre sizes similar to OPC and SF by planetary ball milling at a speed of 400 rpm for 12 hours. The SEM images of the RHA amorphous silica samples after milling are shown in Figure 11. The results indicate that the samples have an uneven particle size distribution ranging from 2 microns to below 100 nm. Figure 11 shows that the two types of amorphous silica corresponding to normal soil RHA and saline soil RHA have similar surface structures and particle sizes, which are smaller and more uniform compared to the two samples corresponding to drought soil RHA and acidic soil RHA. The surface morphology of the four samples is quite similar to the OPC sample shown in Figure 12. In Figure 12, the SEM images of the SF sample reveal spherical particles with a characteristic uneven size distribution. Through analysis of phase structure, surface morphology, and particle size, the suitability of RHA-derived amorphous silica as sustainable SCMs from agricultural by-products is demonstrated. This study contributes to advancing efforts towards sustainable construction practices and the development of resilient infrastructure.

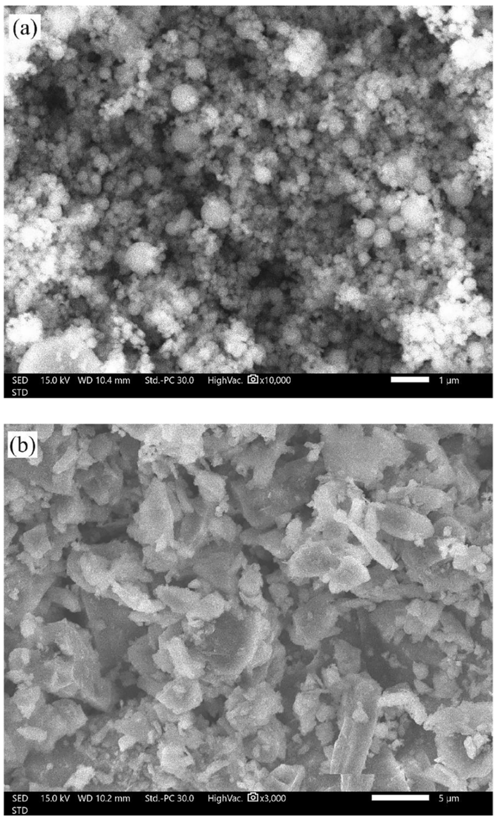

Figure 12. Morphology of: (a) a SF sample and (b) an OPC sample

CONCLUSIONS

Through the analysis of phase structure and surface morphology, the highest efficiency for each type of rice husk under different cultivation conditions was identified. Specifically, at a pyrolysis temperature of 700 °C for 1 hour, the recovery efficiencies for normal soil RHA, saline soil RHA, drought soil RHA, and acidic soil RHA were 87.9%, 96.5%, 94.8%, and 95.6%, respectively. Given the significant fluctuations in soil conditions due to climate change in many rice-producing countries, these results are crucial for selecting appropriate pyrolysis regimes when applying industrial-scale production for amorphous silica from RHA. The study also compared the phase structure, surface morphology, and particle size of RHA-derived amorphous silica, ground to micrometre sizes, with commercial samples of OPC and SF, which are commonly used in the production of construction materials today. The results showed similarities with current commercial products and highlighted the potential of ball milling in controlling the particle size of these RHA-derived amorphous silica samples to the desired size for partially replacing OPC or commercial SCMs like SF.

Acknowledgements

The authors are grateful to the Ministry of Education and Training of Vietnam (MOET) who supported the fund for this research (Grant number: B2022-DHH-15).

REFERENCES

1. Nuaklong P., Jongvivatsakul P., Pothisiri T., Sata V., and Chindaprasirt P. Influence of rice husk ash on mechanical properties and fire resistance of recycled aggregate high-calcium fly ash geopolymer concrete, Journal of Cleaner Production, 2020; 252: 119797. https://doi.org/10.1016/j.jclepro.2019.119797
2. Khan M., Abbas Y., and Fares G. Review of high and ultrahigh performance cementitious composites incorporating various combinations of fibers and ultrafines, Journal of King Saud University-Engineering Sciences, 2017; 29: 339–347. https://doi.org/10.1016/j.jksues.2017.03.006
3. Sani J., Yohanna P., and Chukwujama I. Effect of rice husk ash admixed with treated sisal fibre on properties of lateritic soil as a road construction material, Journal of King Saud University-Engineering Sciences, 2020; 32: 11–18. https://doi.org/10.1016/j.jksues.2018.11.001
4. Rattanachu P., Toolkasikorn P., Tangchirapat W., Chindaprasirt P., and Jaturapitakkul C. Performance of recycled aggregate concrete with rice husk ash as cement binder, Cement and Concrete Composites, 2020; 108: 103533. https://doi.org/10.1016/j.cemconcomp.2020.103533
5. Al-Kutti W., Islam A.S., and Nasir M. Potential use of date palm ash in cement-based materials, Journal of King Saud University-Engineering Sciences, 2019; 31: 26–31. https://doi.org/10.1016/j.jksues.2017.01.004
6. Wang J., Xiao J., Zhang Z., Han K., Hu X., and Jiang F. Action mechanism of rice husk ash and the effect on main performances of cement-based materials: A review, Construction and Building Materials, 2021; 288: 123068. https://doi.org/10.1016/j.conbuildmat.2021.123068
7. Sandhu R.K., Siddique R. Influence of rice husk ash (RHA) on the properties of self-compacting concrete: A review, Construction and Building Materials, 2017; 153: 751–764. https://doi.org/10.1016/j.conbuildmat.2017.07.165
8. Givi A.N., Rashid S., Nora F., Aziz A., Salleh M. Contribution of Rice Husk Ash to the Properties of Mortar and Concrete: A Review, 2010.
9. El-Sayed M.A.and El-Samni T.M. Physical and chemical properties of rice straw ash and its effect on the cement paste produced from different cement types, Journal of King Saud University-Engineering Sciences, 2006; 19: 21–29. https://doi.org/10.1016/S1018-3639(18)30845-6
10. Meddah M., Praveenkumar T., Vijayalakshmi M., Manigandan S., and Arunachalam R. Mechanical and microstructural characterization of rice husk ash and Al2O3 nanoparticles modified cement concrete, Construction and Building Materials, 2020; 255: 119358. https://doi.org/10.1016/j.conbuildmat.2020.119358
11. Cizer Ö., Campforts J., Van Balen K., Elsen J., and Van Gemert D. Hardening of calcium hydroxide and calcium silicate binders due to carbonation and hydration, in International Symposium on Brittle Matrix Composites, Date: 2006/10/23-2006/10/25, Location: Warsaw, Poland, 2006; 589–599.
12. Habeeb G.A. and Mahmud H.B. Study on properties of rice husk ash and its use as cement replacement material, Materials Research, 2010; 13: 185–190. https://doi.org/10.1590/s1516-14392010000200011
13. De Sensale G.R. Effect of rice-husk ash on durability of cementitious materials, Cement and Concrete Composites, 2010; 32: 718–725.
14. Salas A., Delvasto S., de Gutierrez R.M., and Lange D. Comparison of two processes for treating rice husk ash for use in high performance concrete, Cement and concrete research, 2009; 39: 773–778. https://doi.org/10.1016/j.cemconres.2009.05.006
15. Siddika A., Mamun M.A.A., Alyousef R., and Mohammadhosseini H. State-of-the-art-review on rice husk ash: A supplementary cementitious material

in concrete, Journal of King Saud University - Engineering Sciences, 2021; 33: 294–307. https://doi.org/10.1016/j.jksues.2020.10.006

16. Antiohos S., Tapali J., Zervaki M., Sousa-Coutinho J., Tsimas S., and Papadakis V. Low embodied energy cement containing untreated RHA: A strength development and durability study, Construction and Building Materials, 2013; 49: 455–463. https://doi.org/10.1016/j.conbuildmat.2013.08.046
17. Djamaluddin A.R., Caronge M.A., Tjaronge M., Rahim I.R., and Noor N.M. Abrasion resistance and compressive strength of unprocessed rice husk ash concrete, Asian Journal of Civil Engineering, 2018; 19: 867–876.
18. Nzereogu P., Omah A., Ezema F., Iwuoha E., and Nwanya A. Silica extraction from rice husk: Comprehensive review and applications, Hybrid Advances, 2023; 100111. https://doi.org/10.1016/j.hybadv.2023.100111
19. Mboya H.A., King'ondu C.K., Njau K.N., and Mrema A.L. Measurement of pozzolanic activity index of scoria, pumice, and rice husk ash as potential supplementary cementitious materials for Portland cement, Advances in Civil Engineering, 2017; 6952645. https://doi.org/10.1155/2017/6952645
20. Nair D.G., Jagadish K., and Fraaij A. Reactive pozzolanas from rice husk ash: An alternative to cement for rural housing, Cement and Concrete Research, 2006; 36: 1062–1071. https://doi.org/10.1016/j.cemconres.2006.03.012
21. Ahmed A.E. and Adam F. Indium incorporated silica from rice husk and its catalytic activity, Microporous and mesoporous materials, 2007; 103: 284–295. https://doi.org/10.1016/j.micromeso.2007.01.055
22. Alaneme K.K., Ekperusi J.O., and Oke S.R. Corrosion behaviour of thermal cycled aluminium hybrid composites reinforced with rice husk ash and silicon carbide, Journal of King Saud University-Engineering Sciences, 2018; 30: 391: 397. https://doi.org/10.1016/j.jksues.2016.08.001
23. Della V.P., Kühn I., and Hotza D. Rice husk ash as an alternate source for active silica production, Materials letters, 2002; 57: 818–821.
24. Bazargan A., Wang Z., Barford J.P., Saleem J., and McKay G. Optimization of the removal of lignin and silica from rice husks with alkaline peroxide, Journal of Cleaner Production, 2020; 260: 120848. https://doi.org/10.1016/j.jclepro.2020.120848
25. Ghorbani F., Sanati A.M., and Maleki M. Production of silica nanoparticles from rice husk as agricultural waste by environmental friendly technique, Environmental Studies of Persian Gulf, 2015; 2: 56–65.
26. Zou Y. and Yang T. Rice husk, rice husk ash and their applications, in Rice bran and rice bran oil, ed: Elsevier, 2019; 207–246.
27. Nassar M.Y., Ahmed I.S., and Raya M.A. A facile and tunable approach for synthesis of pure silica nanostructures from rice husk for the removal of ciprofloxacin drug from polluted aqueous solutions, Journal of Molecular Liquids, 2019; 282: 251–263, https://doi.org/10.1016/j.molliq.2019.03.017
28. Schlomach J. and Kind M. Investigations on the semi-batch precipitation of silica, Journal of colloid and interface science, 2004; 277: 316–326.
29. Joglekar S.N., Kharkar R.A., Mandavgane S.A., and Kulkarni B.D. Process development of silica extraction from RHA: a cradle to gate environmental impact approach, Environmental Science and Pollution Research, 2019; 26: 492–500. https://doi.org/10.1007/s11356-018-3648-9
30. Costa J.A.S. and Paranhos C.M. Systematic evaluation of amorphous silica production from rice husk ashes, Journal of Cleaner Production, 2018; 192: 688–697. https://doi.org/10.1016/j.jclepro.2018.05.028
31. Numpilai T., Ng K.H., Polsomboon N., Cheng C.K., Donphai W., Chareonpanich M, et al., Hydrothermal synthesis temperature induces sponge-like loose silica structure: A potential support for Fe2O3-based adsorbent in treating As (V)-contaminated water, Chemosphere, 2022; 308: 136267. https://doi.org/10.1016/j.chemosphere.2022.136267
32. Earnshaw A., Greenwood N.N. Chemistry of the Elements Butterworth-Heinemann Oxford, 1997; 60.
33. Bakar R.A., Yahya R., and Gan S.N. Production of High Purity Amorphous Silica from Rice Husk, Procedia Chemistry, 2016; 19: 189–195. https://doi.org/10.1016/j.proche.2016.03.092
34. Atta A., Jibril B., Aderemi B., and Adefila S. Preparation of analcime from local kaolin and rice husk ash, Applied Clay Science, 2012; 61: 8–13. https://doi.org/10.1016/j.clay.2012.02.018
35. Zabihi S.M., Tavakoli H., and Mohseni E. Engineering and microstructural properties of fiber-reinforced rice husk–ash based geopolymer concrete, Journal of Materials in Civil Engineering, 2018; 30: 04018183. https://doi.org/10.1061/(ASCE)MT.1943-5533.0002379
36. H.P.V., P. D.V., T. D.T., P. P.T.T., S. L.V.T., and D.T.N., Effect of pyrolysis process to derive silica from rice husk. Tạp chí Khoa học và công nghệ nông nghiệp Trường Đại học Nông Lâm Huế, 2023; 7: 3729–3737. https://doi.org/10.46826/huaf-jasat.v7n2y2023.1038
37. Bish D.L. and Howard S. Quantitative phase analysis using the Rietveld method, Journal of Applied Crystallography, 1988; 21: 86–91. https://doi.org/10.1107/S0021889887009415
38. C.-L. Hwang and D.-S. Wu, Properties of cement paste containing rice husk ash, Special Publication, 1989; 114: 733–762.
39. Umasabor R. and Okovido J. Fire resistance evaluation of rice husk ash concrete, Heliyon, 2018; 4: e01035. https://doi.org/10.1016/j.heliyon.2018.e01035